IOP Conf. Series: Materials Science and Engineering **389** (2018) 012014 doi:10.1088/1757-899X/389/1/012014

Effect of Oxide Film Crack Length on Film-induced Stress in Stress Corrosion Cracking Tip

YANG Hongliang[1], XUE He[2,*], CUI Yinghao[2] and NI Chenqiang[2]

[1.] Center of Engineering Training, Xi'an University of Science and Technology, Xi'an 710054, China
[2.]School of Mechanical Engineering, Xi'an University of Science and Technology, Xi'an 710054, China

*Corresponding author: Tel: 0086-29-83856250, E-mail: xue_he@hotmail.com

Abstract. Oxide film rupture theory has become one of the most popular models to quantitatively predict the stress corrosion cracking rate at crack tip of Ni-based alloys in high temperature water nuclear environment. To understand the micro-mechanical state at the tip of environment assisted cracking (EAC) without considering the external load, the stress-strain induced by oxide film in the base metal at the EAC tip was simulated and discussed using a commercial finite element analysis code. Results show the stress-strain state induced by oxide film is different because of crack length, and film-induced stress is one of the main factors that can't be ignored in the stress corrosion crack growth driving force. The study also provides a foundation to improve the quantitative predication accuracy of EAC growth rate of nickel-based alloys and austenitic stainless steels in the important structures of nuclear power plants.

1. Introduction

There have been reports on stress corrosion cracking (SCC) in austenitic alloys used in light water reactor (LWR) components over the last thirty years [1,2]. The pressure vessel and the steam generator used in the nuclear power tend to occur stress corrosion in the process of its service, and the surface form a layer of oxide film[3].Usually, the oxide film plays a protective role in stress corrosion. However, under the complex environmental factors, the oxide film can produce film-induced stress, which can promote the dislocation emission and motion, and make the crack tip produce local plastic deformation[4]. The stress can make the intergranular film fracture, leading to the formation of deep matrix crack[5,6]. In the quantitative prediction model of crack growth rate based on slip dissolution theory, crack length is an important mechanical parameter. The crack length will influence the mechanical field of the crack tip induced by film-induced stress[7].In order to understand the effect of crack length on stress and strain field caused by film-induced stress at crack tip, the stress and strain fields in the SCC crack tip were analyzed by using the sub model technology of ABAQUS and the nickel base alloy as the research object. Attempt to obtain effect of crack length on stress and strain field caused by film-induced stress.

2. Theory model

The oxide film rupture theory considers that the EAC process in nickel-based alloys and austenitic stainless steels in high temperature water environment can be divided into two periods: I-oxide film

forming at the crack tip, II-oxide film aging and rupture at the crack tip with a high stress and strain [8,9].

Because the aging and rupture of the oxide film takes most of the time in EAC period, according to the Faraday's law, Ford and Andresen in GE deduced a formula to estimate the EAC growth rate of nickel-based alloys and austenitic stainless steels in high temperature water environment of nuclear power plants[8-10]:

$$\frac{\mathrm{d}a}{\mathrm{d}t}=\frac{M}{Z\rho F}\cdot\frac{i_0}{1-m}\left[\left(\frac{t_0\cdot\dot{\varepsilon}_{ct}}{\varepsilon_f}\right)^m-m\cdot\frac{t_0\cdot\dot{\varepsilon}_{ct}}{\varepsilon_f}\right] \quad (1)$$

Where, da/dt is the EAC growth rate, M and ρ are the atomic mass and the density of metals, respectively, F is Faraday's constant, i_0 is the bare surface oxidation current density, z is the change in charge due to the oxidation process, m is the exponent in the current decay curve, ε_f is the degradation strain of the oxide film, t_0 is the time before onset of the current decay, and dε_{ct} /dt is the strain rate at the EAC tip.

Eq.(1) is the most widely used in prediction equation of the EAC growth rate in nickel-based alloys and austenitic stainless steels in high temperature water environment of nuclear power plants. Fracture mechanism of film-induced stress in stress corrosion cracking can be show as: Without considering the external load, there is an additional tensile stress at one side of the interface matrix. It makes the local plastic deformation at crack tip, and the stress can causes the dislocation emission, which can cause the oxide film intergranular cracking, and then leading to the occurrence and extension of stress corrosion cracking. Thus it can form deep matrix crack, and stress corrosion cracking can be produced[5,6].

3. Finite element modeling

3.1 Specimen model

Half inch compact tension specimen (0.5T-CT) was used in this numerical calculation with the virtual experiment process according to the American Society for Testing and Materials Standard[11]. The geometric shape and size of 0.5T-CT specimen are shown in Figure1. The thickness of the oxide film formed by Ni-based alloys in high temperature and high pressure water is about 1μm to 2 μm [12], and 2 μm is adopted in this research.

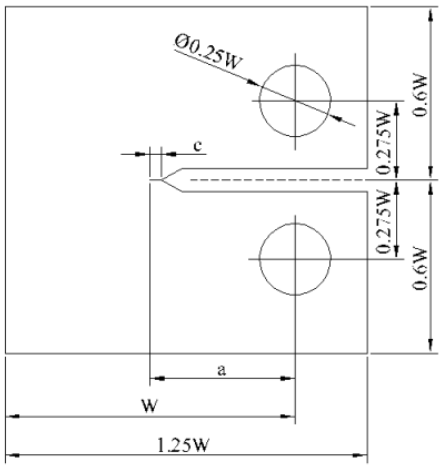

Figure1 Geometric size of 0.5T-CT specimen (W=25mm, a=0.5W, c=2mm)

3.2 Material model

The non linear relationship between stress and strain beyond yield at crack tip of nickel-based alloys is described by Ramberg-Osgood equation in this numerical simulation[13]:

$$\frac{\varepsilon}{\varepsilon_0}=\frac{\sigma}{\sigma_0}+\alpha\left(\frac{\sigma}{\sigma_0}\right)^n \tag{2}$$

Where ε is strain; σ is stress; E is Young's modulus of the material; σ_0 is the yield strength of the material; α is the yield offset and n is the hardening exponent for the plastic.

The material parameters of Ni-based alloys 600 and oxide film are shown in Table 1.

Table 1. Mechanical properties of alloy 600 and the oxide film formed in PWR primary water at 288 ℃ [14,15]

Material	Alloy 600	Oxide film
Young's modulus, E /GPa	189.5	140
Poisson's ratio, ν	0.286	0.31
Yield strength, σ_0 /MPa	436	--
Yield offset, α	3.075	--
Hardening exponent, n	6.495	--

3.3. FE Model

Using ABAQUS sub model to calculate the stress and strain distribution in the SCC crack tip , the base metal and the oxide film are set up as a whole, and the different material properties are given in the modle. Using the plane deformation model and adopting 8 node and the 2 plane strain element, the finite element model is shown in Figure 2.In order to improve the accuracy of the calculation, the oxide film and the base metal at the crack tip are refined to obtain a more detailed and accurate data[16].

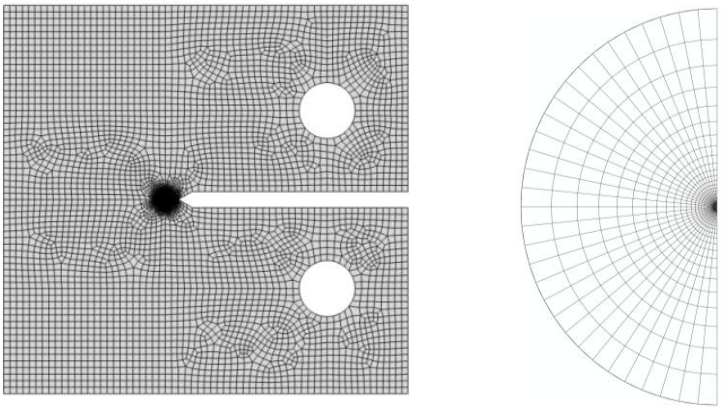

(a) Integral model (b) Crack tip model

Figure 2 Finite element mesh

4. Results and Discussion

4.1. Effect of crack length on Mises stress

Figure 3 shows the influence of crack length on the Mises stress induced by film-induced stress around the crack tip. When a=0, the Mises stress have the maximum values at θ=0° and decrease gradually as θ increase, and the smallest value appears at θ=90°. When a>0, Mises stress changes most dramatically in the range of about -30°～30°. Stress concentration phenomenon occurs because of the

existence of the crack, and the maximum value of Mises stress occurs at θ=0°. When the crack is initially formed in the oxide film, the Mises stress is gradually increased with the increasing of the crack length. When the crack is extended to the Ni-based alloys, the Mises stress decreases slightly with the increasing of the crack length. This is due to the existence of the crack, the film-induced stress is released, and the stress on the crack tip is reduced.

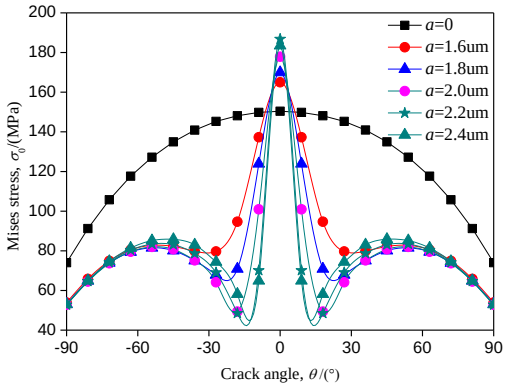

Figure 3 Effect of crack length on Mises stress

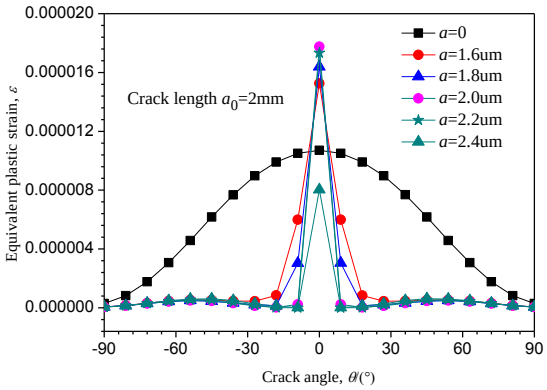

Figure 4 Effect of crack length on equivalent plastic strain

4.2. Effect of crack length on equivalent plastic strain

Figure 4 shows the effect of crack length on equivalent plastic strain induced by film-induced stress around the crack tip. When a=0, the equivalent plastic strain have the maximum values at θ=0° and decrease gradually as θ increase, and the smallest value appears at θ=90°. When a>0, equivalent plastic strain changes most dramatically in the range of about -30°～30°, and the maximum value of equivalent plastic strain occurs at θ=0° because of stress concentration phenomenon. When the crack is initially formed in the oxide film, equivalent plastic strain is gradually increased with the increasing of the crack length. When the crack is extended to the Ni-based alloys, the equivalent plastic strain decreases sharply with the increasing of the crack length because of the film-induced stress is released.

4.3 Effect of crack length on tensile stress

The effect of crack length on tensile stress induced by film-induced stress around the crack tip is shown in Figure 5. When a=0, the tensile stress have the maximum values at θ=0° and decrease to negative gradually as θ increase, and the tensile stress is changed from tensile stress to compressive stress. When a>0, tensile stress changes sharply in the range of about -30°～30°, and the maximum value of tensile stress occurs at θ=0°. The tensile stress is changed into compressive stress with the increase of crack length when the crack is extended to the Ni-based alloys.

4.4. Effect of crack length on tensile plastic strain

The effect of crack length on tensile plastic strain induced by film-induced stress around the crack tip is shown in Figure 6. When a=0, the tensile plastic strain have the maximum values at θ=0° and decrease to negative gradually as θ increase. When a>0, tensile plastic strain changes sharply in the range of about -30°～30°, and the maximum value of tensile stress occurs at θ=0°. When the crack is initially formed in the oxide film, tensile plastic strain is slightly increased with the increasing of the crack length. When the crack is extended to the Ni-based alloys, the tensile plastic strain decreases clearly with the increasing of the crack length.

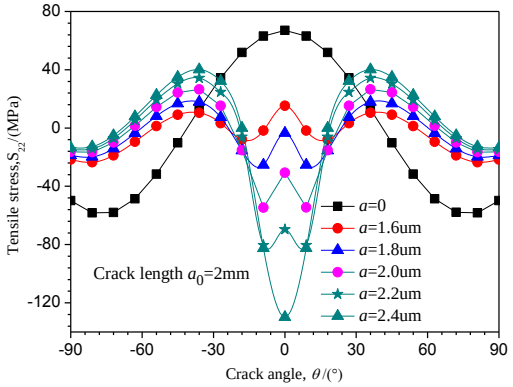

Figure 5 Effect of crack length on tensile stress

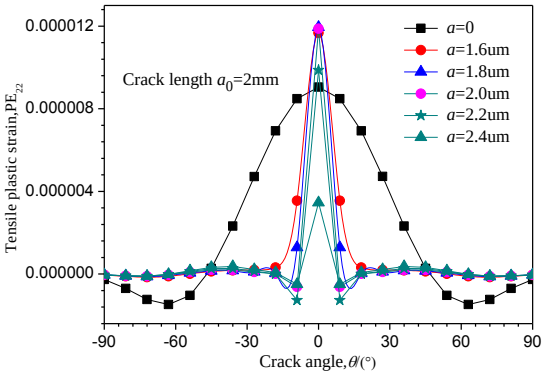

Figure 6 Effect of crack length on tensile plastic strain

4.5 Effect of crack length on tensile plastic strain gradient

Xue et al[17] proposed a method to replace the crack tip strain rate by using the crack tip strain gradient. In the strain gradient model, it is assumed that the crack tip strain is equal to the plastic strain at the front of the crack tip. In order to calculate conveniently, the crack tip strain gradient can be calculated by simplified formula (3).

$$\frac{d\varepsilon_p}{da} \approx \frac{\Delta\varepsilon_p}{\Delta a} = \frac{\varepsilon_{p2} - \varepsilon_{p1}}{a_{i+1} - a_i} \tag{3}$$

Figure 7 shows the effect of crack length on tensile plastic strain gradient at crack tip. When the crack grows inside the oxide film, tensile strain rate is negative. the tensile plastic strain gradient is gradually increased with the increasing of the crack length. When the crack is extended to the Ni-based alloys, the tensile plastic strain gradient increases with the increasing of the crack length at $r<$ 0.4μm, and the tensile plastic strain gradient gradually approaches to 0 with the increase of r.

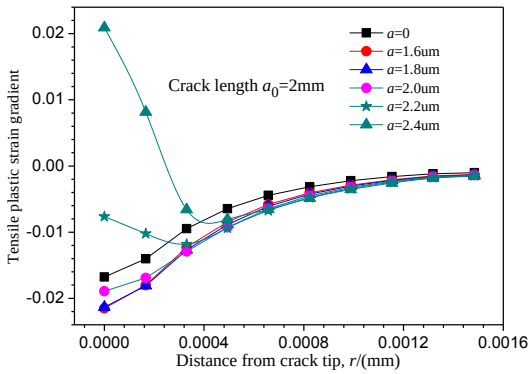

Figure 7 Effect of crack length on tensile plastic strain gradient at crack tip

5. Conclusion

(1) The change of stress and strain is obvious in the range of about -30 °~30 °, and the maximum value of stress and strain occurs at θ=0 °. When the crack is initially formed in the oxide film, stress and strain gradually increase with the increasing of the crack length. When the crack is extended to the Ni-based alloys, the stress and strain decreases with the increasing of the crack length.

(2) Without considering the external load, the effective stress of the crack increases with the increasing of film-induced, and promotes the effective of plastic strain. When the critical condition is reached, the nucleation and expansion of micro cracks are caused, which leads to stress corrosion cracking. Film-induced stress is one of the main factors that can't be ignored in the driving force of stress corrosion crack growth.

Acknowledgments
Foundation item: National Natural Science Foundation of China (51475362), Scientific Research Program Funded by Shaanxi Provincial Education Department (16JK1493)

References

[1] Seiya Yamazaki, Zhanpeng Lu, Yuzuru Ito et al. The effect of prior deformation on stress corrosion cracking growth rates of Alloy 600 materials in a simulated pressurized water reactor primary water[J], Corrosion Science, 2008, 50(3) 835–846.
[2] R.W. Staehle. 1-Historical views on stress corrosion cracking of nickel-based alloys : The Coriou effect[J]. Stress Corrosion Cracking of Nickel Based Alloys in Water-cooled Nuclear Reactors, 2016:3-131.
[3] WANG Wenwen, LUO Ji, GUO Leichen, et al. Finite element analysis of stress corrosion cracking for copper in an ammoniacal solution [J]. Rare Metals, 2015, 34(6): 426-430.
[4] Chu Wuyang, Qiao Lijie. Hydrogen embrittlement and stress corrosion -- basic part [M]. 2013.
[5] Hong Lu, Kewei Gao, Wuyang Chu. Determination of tensile stress induced by dezincification layer during corrosion for brass[J]. Corrosion Science, 1998, 40(10):1663-1670.
[6] Guo X J, Gao K W, Qiao L J, et al. The correspondence between susceptibility to SCC of brass and corrosion-induced tensile stress with various pH values[J]. Acta Metallrugica Sinica, 2002, 44(10):2367-2378.
[7] Han Enhou, Wang Jianqiu, Wu Xinqiang. Corrosion Mechanisms of Stainless Steel and Nickel Base Alloys in High Temprature High Pressure Water[J]. Acta Metallurgica Sinica, 2010, 46(11): 1379-1390.
[8] Tetsuo Shoji, Zhanpeng Lu, Hiroyoshi Murakami. Formulating stress corrosion cracking growth rates by combination of crack tip mechanics and crack tip oxidation kinetics[J]. Corrosion Science, 2010, 52(3): 769-779.
[9] Peter L Andresen, F. Peter Ford. Fundamental modeling of environmental cracking for improved design and lifetime evaluation in BWRs[J]. International Journal of Pressure Vessel Technology, 1994, 59(1--3): 61-70.
[10] Peter L. Andresen, F. Peter Ford. Response to " On the modeling of stress corrosion cracking of iron and nickel base alloys in high temperature aqueous environments" [J]. Corrosion Science, 1996, 38(6): 1011-1016.
[11] ASTM standard E399-90, 2002. Annual Book of ASTM Standards [S].
[12] YANG Hongliang, XUE He, ZHAO Lingyan et al. Effect of Oxide Film Shape on Stress-Strain at Stress Corrosion Cracking Tip of Ni-Based Alloy[J]. Hot Working Technology. 2016, 45(20): 58-60.
[13] Ramberg W, Osgood W R. Description of stress-strain curves by three parameters. NACA Tech Note[R], No. 902, 1943.
[14] P.Goudeau, P.O.Renault, P.Villain, C.Coupeau. Thin Solid Films[J], 2001, 496-500.
[15] Yang Hongliang, Xue He, Yang Fuqiang, Zhao Lingyan. Effect of Film-Induced Stress on Mechanical Properties at Stress Corrosion Cracking Tip[J]. Rare Metal Materials and Engineering, 46(2017): 3595-3600.
[16] YANG Hongliang, XUE He, YANG Fan. Study on Oxide Film Rupture Behavior Caused by Film-induced Stress[J]. FOUNDRY TECHNOLOGY, 38(6): 1274-1277.
[17] Xue H, Sato Y, Shoji T. Quantitative estimation of the growth of environmentally assisted cracks at flaws in light water reactor components[J]. Journal of Pressure Vessel and Technology: Transactions of the ASME, 2009, 131(1):61-70.